DMS: DIFFERENTIABLE DIMENSION SEARCH FOR BINARY NEURAL NETWORKS

Anonymous authors
Paper under double-blind review

ABSTRACT

Binary Neural Networks (BNN) have been widely explored in the field of the efficient and accelerated deep learning area. However, since the inherent essence of BNN brings intensive oscillation in training and validation (Zhu et al., 2019), existing methods either seek new optimization methods or increase bit-width to bridge the gap to the full precision models. In this work, we focus on determining the dimension (i.e. number of weights or kernels) for BNN. We conjecture that the optimal dimension (channels) can be viewed as a continuous logistic random variable, then we use the differentiable Neural Architecture Search (NAS) method to learn the distribution of this variate. Though the search space is defined over thousands for a single convolution layer, our method is efficient and able to reduce the search complexity from $\mathcal{O}(N)$ to $\mathcal{O}(1)$. Extensive experiments on CIFAR10 and ImageNet dataset validate the effectiveness of the proposed algorithm.

1 INTRODUCTION

Studies of Quantization Neural Network (QNN) (Hubara et al., 2017) aim to lower the energy consumption, latency and memory cost when deep neural networks are deployed to resource-limited devices (e.g., mobile phones and embedded devices). BNN is the most promising approach for hardware performance, which brings 32$\times$ memory saving and about 58$\times$ computation acceleration on CPU (Rastegari et al., 2016). However, the performance (accuracy) of BNN in a large-scale task, such as ImageNet classification, still suffers from severe degradation from the full precision model. Kim et al. (2020) reach state-of-the-art BNN accuracy on ResNet-18 (He et al., 2016), which still degrades 10% top-1 accuracy from the full precision models. The task of designing an effective optimization method to find a better local optimum of BNN is highly non-trivial (Zhu et al., 2019). Another solution is to increase bit-width in QNN, where both uniform precision network (Zhou et al., 2016; Jung et al., 2019; Li et al., 2020) and mixed precision network (Wang et al., 2019) are studied.

Instead of neither finding better optimization methods nor increase the bit-width, the scope of this research work lies in the high-dimension space (i.e. the number and size of kernels) in BNN. Kanerva (2009) points that two high-dimensional vectors of dimension d whose entries are chosen uniformly from the set $\{-1, +1\}$ are approximately orthogonal. Anderson & Berg (2018) shows that in high dimension space the angle between a Gaussian vector and its binary vector can be small when dimension increases. Such theoretical results indicate that BNN can benefit from higher dimension.

Wide ResNet (Zagoruyko & Komodakis, 2016) and Wide Reduced Precision Network (Mishra et al., 2018) manually increase the width (channel number) and shows that performance can be improved along with the dimension in both full precision networks and QNNs. Intuitively, each layer in CNN can have different optimal channels for a certain architecture. Recently, NAS (Zoph & Le, 2016) algorithm is thrived to obtain a state-of-the-art architecture. Most NAS research works (Pham et al., 2018; Zoph et al., 2018; Real et al., 2019; Liu et al., 2018; Cai et al., 2018) focus on determining the architecture with a deterministic channel number. One problem is that the search space for channels can be huge (from 16 to 4k) and it will grow exponentially with layers. Shen et al. (2019) use evolution algorithm to search the channel numbers in BNN, however, they only search 6 expansion ratios for each layer, which causes suboptimal results. DAS (Shin et al., 2018) leverages the linearity of convolution (i.e., multiple convolutions can be fused into one convolution) to search the layer hyper-parameters in full precision model, yet it is still not practical to search the thousands of consecutive

channels together. We propose DMS (Differentiable diMension Search) to address this issue. In Sect. 2, we show the details of the DMS algorithm. In Sect. 3 we conduct several experiments on CIFAR10 and ImageNet dataset.

2 Differentiable Dimension Search

2.1 Preliminaries

Suppose weights in a convolutional layer are represented by a 4D tensor $\boldsymbol{W} \in \mathbb{R}^{c_{\text{out}} \times c_{\text{in}} \times k \times k}$, where c_{in} and c_{out} denote the input and the output channel of the layer, and k indicates the squared kernel size. Activations are denoted by tensor $\boldsymbol{X}$. In BNN, the weights as well as activations are binarized as follows

$$\boldsymbol{w}^b = \text{sign}(\boldsymbol{w}) \times \mathbb{E}[|\boldsymbol{w}|], \tag{1}$$

$$\boldsymbol{X}^b = \alpha \times \text{round}(\text{clip}(\boldsymbol{X}/\alpha, 0, 1)), \tag{2}$$

where $\boldsymbol{w}$ is a convolutonal kernel, α is the learnable quantization step size for activations. Eq. 2 rounds $\boldsymbol{X}$ to $\{0, \alpha\}$. Our task is to find an optimal c_{out} for each layer.* Following Shen et al. (2019), we use channels times an expansion ratio r to denote the final channel number in the architecture. However, they only define 6 candidate value for expansion ratio in search space, which is suboptimal.

Consider the search space $\mathcal{R}$ where any $r \cdot c_{\text{out}} \in \mathcal{R}$ is a positive integer. In DARTS (Liu et al., 2018), the forward propagation of a node in the directed acyclic graph (DAG) is computed by

$$\boldsymbol{O} = \sum_{r_i \in \mathcal{R}} \frac{\exp(\gamma_i)}{\sum_{r_j \in \mathcal{R}} \exp(\gamma_j)} (\boldsymbol{W}_i^b * \boldsymbol{X}^b), \tag{3}$$

where γ_i is the strength for the channel choice i and $\boldsymbol{W}_i \in \mathbb{R}^{r_i \cdot c_{\text{out}} \times c_{\text{in}} \times k \times k}$. Unfortunately, differentibale method require $\mathcal{O}(N)$ GPU memory to retain the graph nodes, and the search space in this task could be huge. For example, consider the original channel $c_{\text{out}} = 256$, the expansion ratio takes from 0.1 to 4, then, there could near 1000 choices, which is not hardware-friendly.

2.2 Search Space

Our work is inspired by Louizos et al. (2019), where the weights are added with a noise and thus can be stochastically quantized. In Eq. 3, we notice that the channel numbers may be discrete, but all candidate choices are consecutive integers, which indicates that we do not need to use softmax to relax the discrete space. We conjecture that the optimal expansion ratio lies in a small range, (i.e., several consecutive candidates yield optimal results) whereas the other range in the search space is less favorable for the architecture. To model this probability among the search space, we first set the expansion ratio as a continuous random variable r and let it follow a Logistic distribution $L(\mu, \sigma)$. Given a certain distribution of the expansion ratio, we can calculate the probability in a continuous range. To calculate the probability of a candidate r_i, we use the Cumulative Density Function (CDF) of the distribution over the range that around this discrete candidate.

$$p_i(\text{r} = r_i | \text{r} \sim L(\mu, \sigma)) = \text{CDF}(r_i + \Delta) - \text{CDF}(r_i - \Delta) = \frac{1}{1 + e^{((r_i + \Delta - \mu)/\sigma)}} - \frac{1}{1 + e^{((r_i - \Delta - \mu)/\sigma)}}, \tag{4}$$

where $\Delta = 0.5/c_{\text{out}}$ is the half step size between two expansion ration in the search space. In the search space, we want to measure the probability of being selected. First, let r_0 and r_m (where $m = |\mathcal{R}|$ and can be $+\infty$) be the least and largest expansion ration in $\mathcal{R}$. Then we can compute the marginal probability by

$$\hat{p}_i(\text{r} = r_i | \text{r} \in (r_0 - \Delta, r_m + \Delta)) = \frac{\text{CDF}(r_i + \Delta) - \text{CDF}(r_i + \Delta)}{\text{CDF}(r_m + \Delta) - \text{CDF}(r_0 - \Delta)}, \tag{5}$$

where $\sum_{r_i \in \mathcal{R}} \hat{p}_i = 1$. Fig. 1a illustrates the process that the continuous Logistic distribution becomes categorical distribution.

*Our method can also find the optimal kernel size and groups, we leave those in the future work.

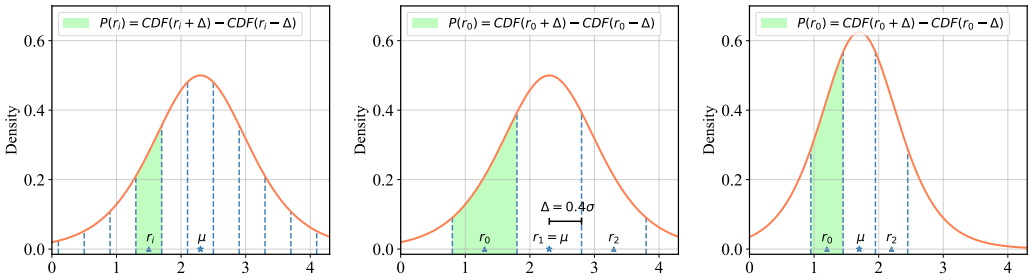

(a) Logistic search space (b) clustered search space (c) clustered search space

Figure 1: **Left:** the categorical probability of r_i is the probability over a continous range. **Middle:** the search space has been clustered to only 3 representative expansion ratio, which reduces the search complexity. **Right:** after epochs of training, we reduce the variance of the distribution to narrow the range that contains optimal expansion ratio.

2.3 Candidate Clustering

Unfortunately, even we can get the categorical probability of each candidate expansion ratio under the Logistic distribution. The search complexity is still $\mathcal{O}(N)$ because we have to compute each convolution in backward (Cai et al., 2018). Therefore, we cluster all candidates to only 3 representative candidates in the search space. The intuition is that since the channels are consecutive integers, it is unnecessary strictly choose one candidate in forward. One candidate can share the same probability with its neighbors. In our experiments, we use 3 candidates in search space with $\mathcal{R}_c = \{\mu, \mu + 0.8\sigma, \mu - 0.8\sigma\}$, and we find they are sufficient enough to represent the search space. Fig. 1b shows the clustered candidate in the search space, where the search complexity is reduced to $\mathcal{O}(1)$. To calculate the probability of each candidate, we set $\Delta = 0.4 \cdot \sigma$ in Eq. 5.

In the clustered search space, the σ controls the variance of the distribution as well as the variance of the candidates. Therefore, we initialize σ to slightly high variance distribution so that the search space can cover a broad range in the search space. During training, we progressively decrease the value of σ, since we want to restraint the optimal channel range in a relatively small range as shown in Fig. 1c.

2.4 Optimization

We use the binarized path for computing the feature maps like Cai et al. (2018), i.e., given the probability of each choice, we randomly sample one path in the forward pass. However, sampling from a categorical distribution is not differentiable. Here Gumbel-Softmax trick (Jang et al., 2016; Maddison et al., 2016) is applied to make sure gradients can flow to the distribution:

$$\boldsymbol{O} = \sum_{r_i \in \mathcal{R}_c} \frac{\exp((\log \hat{p}_i + g_i)/\tau)}{\sum_{r_j \in \mathcal{R}_c} \exp((\log \hat{p}_j + g_j)/\tau)} (\boldsymbol{W}_i^b * \boldsymbol{X}^b), \text{ where } g_i \sim \text{Gumbel}(0, 1). \tag{6}$$

τ is called temperature and controls the tightness of the softmax function. We use the same bilevel optimization problem (Liu et al., 2018) and use alternative method to optimize architecture parameters (expansion ratio) and weights. Since increasing channels for BNN will lead to greater latency and model size, we add hardware penalties in the optimization objective. Denote $\mathcal{L}_{\text{train}}$, $\mathcal{L}_{\text{valid}}$ as the training loss and the validation loss. we formulate the bilevel optimization problem as follows:

$$\min_{\mu} \ \mathcal{L}_{\text{valid}}(w^{b*}(\mu, \sigma), \mu) + \lambda \max(0, \text{Memory} - \text{Memory}_{target}), \tag{7}$$

$$\text{s.t.} \ \ w^{b*}(\mu, \sigma) = \arg\min_{w^b} \ \mathcal{L}_{\text{train}}(w^b, \mu), \tag{8}$$

where w^b indicates the binary weights in BNN, λ is the tradeoff parameter for hardware performances. Higher λ as well as lower Memory_{target} result in less parameter numbers but the accuracy may degrade and vice versa. In particular, we optimize the distribution ($L(\mu, \sigma)$) of expansion ratio. Unlike ProxylessNAS where only two candidates will be updated in the search space, all candidates in the search space can be updated after updating μ and adjusting σ while the search complexity can

Table 1: Accuracy and model size comparison between uniformly wide BNN and our DMS architecture on VGG-11 and ResNet-18.

Models	**VGG-11 CIFAR10**			**Res-18 CIFAR10**			**Res-18 ImageNet**			
	Params	Saving	Acc.-1	Params	Saving	Acc.-1	Params	Saving	Acc.-1	Acc.-5
Full Prec.	2.20 MB	1×	88.10	2.67 MB	1×	92.75	44.5 MB	1×	69.6	89.2
BNN 1×	0.08 MB	27×	78.31	0.09 MB	29×	85.33	3.29 MB	13.5×	52.77	76.85
BNN 2×	0.29 MB	7.6×	85.37	0.40 MB	6.7×	90.25	9.24 MB	4.8×	64.00	85.45
BNN 3×	0.65 MB	3.4×	88.17	0.98 MB	2.7×	92.25	17.8 MB	2.5×	68.51	88.25
BNN 4×	1.14 MB	1.9×	88.68	1.92 MB	1.4×	93.01	29.1 MB	1.5×	70.35	89.27
DMS-A	**0.08 MB**	27×	**84.16**	**0.10 MB**	27×	**89.32**				
DMS-B	**0.64 MB**	2.6×	**89.10**	**0.84 MB**	3.2×	**92.70**				

still be reduced to $\mathcal{O}(1)$. In architecture evaluation, we choose the mean of the distribution μ as the optimal expansion ratio for BNNs.

However, whenever μ is updated, the search space will change accordingly, which means the computation graph (including weights) we trained before is no longer retained and the network has to be trained from scratch. To extenuate such a problem, we use several methods: First, we do not alternatively optimize $\mathcal{L}_{\text{train}}$ and $\mathcal{L}_{\text{valid}}$ for each batch iteration like DARTS but for several epochs. Second, we use cosine annealing learning rate (Loshchilov & Hutter, 2016) to accelerate the convergence of the weights when descending $\mathcal{L}_{\text{train}}$. Last but most important, we use warm restarts for w^b after updating μ. We only intercept the first corresponding weights of the last trained model. We call this as best effort initialization. Please refer to the detailed algorithm in Appendix. A.

3 Experiments

3.1 CIFAR10

We test our DMS algorithm on two architecture channels for CIFAR10 dataset, VGG-11 (Simonyan & Zisserman, 2014) and ResNet-18 (He et al., 2016). Note that we keep other layer architecture (kernel size) the same except for the channel numbers. ResNet and VGG for CIFAR10 has only 1/4 channels of those for ImageNet. We compare the accuracy and the model size in full precision model, BNN (with uniform expansion ration) model. We put the detailed implementation in the Appendix. The results are shown in Table 1 from which we can see that directly binarize the full precision original model could result in a severely degraded neural network. On ResNet-18, BNN (without channel expansion) only achieves 85.33% accuracy, which is 7.42% less than the full precision counterparts. When uniformly expand the channel to 2 times greater or even 4 times greater, the accuracy will approach to the full precision one.

However, not all layers need expanding their channels. We first show DMS-A, where we set a relatively large penalty for model size, the model size is on par with the ordinary architecture, demonstrating our DMS algorithm can prune some redundant channels. DMS-A achieves almost the same accuracy of BNN 2× with **3.6**× less model size in VGG-11. DMS-B has less penalty for model size, we show that DMS-B for ResNet-18 is on par with the full precision accuracy while still shares a 3.2× compression ratio. The channel distribution for each layer is reported in Fig. 4.

3.2 ImageNet

We highlight our search algorithm is efficient since the search space is clusterd, therefore no proxy model is need for large scale dataset like ImageNet. Due to time limit, we directly use the expansion ratio trained in CIFAR10 for now. From Table 1 we notice that

In the future, we plan to directly search channels on ImageNet.

REFERENCES

Alexander G. Anderson and Cory P. Berg. The high-dimensional geometry of binary neural networks. In *International Conference on Learning Representations*, 2018. URL https://openreview.net/forum?id=B1IDRdeCW.

Han Cai, Ligeng Zhu, and Song Han. Proxylessnas: Direct neural architecture search on target task and hardware. *arXiv preprint arXiv:1812.00332*, 2018.

Kaiming He, Xiangyu Zhang, Shaoqing Ren, and Jian Sun. Deep residual learning for image recognition. In *Proceedings of the IEEE conference on computer vision and pattern recognition*, pp. 770–778, 2016.

Yihui He, Xiangyu Zhang, and Jian Sun. Channel pruning for accelerating very deep neural networks. In *Proceedings of the IEEE International Conference on Computer Vision*, pp. 1389–1397, 2017.

Itay Hubara, Matthieu Courbariaux, Daniel Soudry, Ran El-Yaniv, and Yoshua Bengio. Quantized neural networks: Training neural networks with low precision weights and activations. *The Journal of Machine Learning Research*, 18(1):6869–6898, 2017.

Eric Jang, Shixiang Gu, and Ben Poole. Categorical reparameterization with gumbel-softmax. *arXiv preprint arXiv:1611.01144*, 2016.

Sangil Jung, Changyong Son, Seohyung Lee, Jinwoo Son, Jae-Joon Han, Youngjun Kwak, Sung Ju Hwang, and Changkyu Choi. Learning to quantize deep networks by optimizing quantization intervals with task loss. In *Proceedings of the IEEE Conference on Computer Vision and Pattern Recognition*, pp. 4350–4359, 2019.

Pentti Kanerva. Hyperdimensional computing: An introduction to computing in distributed representation with high-dimensional random vectors. *Cognitive computation*, 1(2):139–159, 2009.

Hyungjun Kim, Kyungsu Kim, Jinseok Kim, and Jae-Joon Kim. Binaryduo: Reducing gradient mismatch in binary activation network by coupling binary activations. In *International Conference on Learning Representations*, 2020. URL https://openreview.net/forum?id=r1x0lxrFPS.

Diederik P Kingma and Jimmy Ba. Adam: A method for stochastic optimization. *arXiv preprint arXiv:1412.6980*, 2014.

Yuhang Li, Xin Dong, and Wei Wang. Additive powers-of-two quantization: An efficient non-uniform discretization for neural networks. In *International Conference on Learning Representations*, 2020. URL https://openreview.net/forum?id=BkgXT24tDS.

Hanxiao Liu, Karen Simonyan, and Yiming Yang. Darts: Differentiable architecture search. *arXiv preprint arXiv:1806.09055*, 2018.

Ilya Loshchilov and Frank Hutter. Sgdr: Stochastic gradient descent with warm restarts. *arXiv preprint arXiv:1608.03983*, 2016.

Christos Louizos, Matthias Reisser, Tijmen Blankevoort, Efstratios Gavves, and Max Welling. Relaxed quantization for discretized neural networks. In *International Conference on Learning Representations*, 2019. URL https://openreview.net/forum?id=HkxjYoCqKX.

Chris J Maddison, Andriy Mnih, and Yee Whye Teh. The concrete distribution: A continuous relaxation of discrete random variables. *arXiv preprint arXiv:1611.00712*, 2016.

Asit Mishra, Eriko Nurvitadhi, Jeffrey J Cook, and Debbie Marr. WRPN: Wide reduced-precision networks. In *International Conference on Learning Representations*, 2018. URL https://openreview.net/forum?id=B1ZvaaeAZ.

Hieu Pham, Melody Y Guan, Barret Zoph, Quoc V Le, and Jeff Dean. Efficient neural architecture search via parameter sharing. *arXiv preprint arXiv:1802.03268*, 2018.

Siyuan Qiao, Huiyu Wang, Chenxi Liu, Wei Shen, and Alan Yuille. Weight standardization. *arXiv preprint arXiv:1903.10520*, 2019.

Mohammad Rastegari, Vicente Ordonez, Joseph Redmon, and Ali Farhadi. Xnor-net: Imagenet classification using binary convolutional neural networks. In *European conference on computer vision*, pp. 525–542. Springer, 2016.

Esteban Real, Alok Aggarwal, Yanping Huang, and Quoc V Le. Regularized evolution for image classifier architecture search. In *Proceedings of the aaai conference on artificial intelligence*, volume 33, pp. 4780–4789, 2019.

Mingzhu Shen, Kai Han, Chunjing Xu, and Yunhe Wang. Searching for accurate binary neural architectures. In *Proceedings of the IEEE International Conference on Computer Vision Workshops*, pp. 0–0, 2019.

Richard Shin, Charles Packer, and Dawn Song. Differentiable neural network architecture search, 2018. URL https://openreview.net/forum?id=BJ-MRKkwG.

Karen Simonyan and Andrew Zisserman. Very deep convolutional networks for large-scale image recognition. *arXiv preprint arXiv:1409.1556*, 2014.

Kuan Wang, Zhijian Liu, Yujun Lin, Ji Lin, and Song Han. Haq: Hardware-aware automated quantization with mixed precision. In *IEEE Conference on Computer Vision and Pattern Recognition (CVPR)*, 2019.

Sergey Zagoruyko and Nikos Komodakis. Wide residual networks. *arXiv preprint arXiv:1605.07146*, 2016.

Shuchang Zhou, Yuxin Wu, Zekun Ni, Xinyu Zhou, He Wen, and Yuheng Zou. Dorefa-net: Training low bitwidth convolutional neural networks with low bitwidth gradients. *arXiv preprint arXiv:1606.06160*, 2016.

Shilin Zhu, Xin Dong, and Hao Su. Binary ensemble neural network: More bits per network or more networks per bit? In *Proceedings of the IEEE Conference on Computer Vision and Pattern Recognition*, pp. 4923–4932, 2019.

Barret Zoph and Quoc V Le. Neural architecture search with reinforcement learning. *arXiv preprint arXiv:1611.01578*, 2016.

Barret Zoph, Vijay Vasudevan, Jonathon Shlens, and Quoc V Le. Learning transferable architectures for scalable image recognition. In *Proceedings of the IEEE conference on computer vision and pattern recognition*, pp. 8697–8710, 2018.

Algorithm 1: Search Algorithm for DMS.

Input: Initial distribution μ_0, σ_0 for BNN; Total training epoch T ; training set and validation set.

for *all* $i = 1, 2, \ldots, T$-*epoch* **do**
  Cluster candidates and construct a specific architecture $w^b(\mu, \sigma)$;
  if *Previous states exists* **then**
    Best Effort Initialization($w^b(\mu, \sigma)$, *Previous states*);
  Get training set data;
  for *all* $j = 1, 2, \ldots, T'$-*epoch* **do**
    Descending $\mathcal{L}_{\text{train}}$ and update $w^b(\mu, \sigma)$ with training set;
    Cosine annealing learning rate η;
  Get validation set data;
  Descending $\mathcal{L}_{\text{valid}}$ and update μ with validation set;
  Previous states = $w^b(\mu, \sigma)$;
  Deflate σ with a multiplier β.
return optimized μ ;

A Optimization Details

A.1 Algorithm

Alg. 1 illustrates the search algorithm of DMS. Our search algorithm is different from that of DARTS (Liu et al., 2018) as a result of the dynamic DAG. First, we update $w^b(\mu, \sigma)$ for T' epochs to get a closer approximation for w^{b*}. In each epoch, we use cosine annealing learning rate to accelerate the convergence. After updating μ and before we sample a new architecture from the distribution $L(\mu, \sigma)$, we first store the weights and then use best effort initialization to warm restart the weights in the sampled architecture. In particular, denote the w^{t-1} as the stored weights in the previous architecture and w^t weights in the new architecture. We initialize them as follows:

- if $\textit{dim}(w^{t-1}) > \textit{dim}(w^t)$, we intercept the first corresponding weights. i.e.,
$$w^t[:] = w^{t-1}[0 : \textit{dim}(w^{t-1})] \tag{9}$$
- if $\textit{dim}(w^{t-1}) \leq \textit{dim}(w^t)$, we could only initialize the first corresponding dimension in w^t:
$$w^t[0 : \textit{dim}(w^{t-1})] = w^{t-1}[:] \tag{10}$$

Though we could not restarts completely from the previous weights, the discrepancy will become smaller when learning rate and variance of the distribution is downscaled. We show our best effort initialization is crucial for the convergence of the model in Sect. B.1.

A.2 Linearity of Convolution

We use the linearity of the convolution in Eq. 6, i.e., the weights are added first is equal to adding the feature map:

$$\boldsymbol{O} = \sum_{r_i \in \mathcal{R}_c} (\pi_i \boldsymbol{W}_i) * \boldsymbol{X} = \sum_{r_i \in \mathcal{R}_c} (\pi_i \boldsymbol{W}_i * \boldsymbol{X}), \tag{11}$$

where π_i is the sample from the Gumbel-Softmax distribution. Only one convolution is computed for one node. For weights with different channels, we pad the rest channels with zeros to highest dimension. Given the validation loss $\mathcal{L}_{\text{valid}}$, we can compute the gradients as using: $\frac{\partial \mathcal{L}_{\text{valid}}}{\partial \mu} = \sum_{i \in \mathcal{R}_c} \frac{\partial \mathcal{L}_{\text{valid}}}{\partial \hat{p}_i} \frac{\partial \hat{p}_i}{\partial \mu}$.

A.3 ResNet Architecture

To compare with full precision ResNets (He et al., 2016), and the uniformly wide BNN, we do not modify the architecture except for the channel numbers. Therefore, to keep residual connections

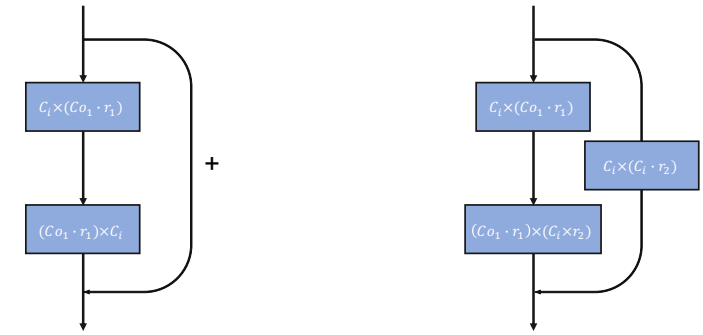

(a) ResBlk without downsample layer (b) ResBlk with downsample layer

Figure 2: ResNet architecture in DMS.

intact, the input and output channel of a residual block should be kept the same. Shown in Fig. 2, we only set 1 expansion ratio for one residual block in an effort to keep the skip connections. For the blocks that have downsample layer, it is reasonable to allocate a learnable expansion ratio r_2 to the second convolutional layer.

B Experiments Details

B.1 Convergence

As aforementioned, DAG is dynamic during searching since either updating μ or adjusting σ leads to the change of search space. Therefore, we propose best effort initialization (BEI) to warm restart the sampled architecture. In Fig. 3, we compare the training error if the BEI is applied. Though the after the initialization the training error is raised, the newly sampled architecture is not trained from scratch like 3b. After only few epochs of training, the training error can reach the lowest in history and thus can continue to be optimized. Without BEI, the final distribution of expansion ratio may not be suitable for BNNs since every time its input is not the optimal weights.

Next, we evaluate the accuracy of searched architecture (ResNet-18-A with or without BEI). DMS-A with BEI gets 89.30% accuracy and DMS-A without BEI gets 87.74% accuracy, demonstrating warm restarts is crucial for our method. Our results show that weights sharing (or maintenance) in differentiable method is necessary.

B.2 Implementation

We use PyTorch to implement our DMS algorithm. Our search code and evaluation code are released anonymously at https://github.com/codes4paper/DMS_for_BNN.

B.2.1 Network Search

For VGG-11 and ResNet-18, we do not modify any layer numbers and hyper-parameters (e.g., kernel size, padding, group) except for channel numbers. The original channels for CIFAR10 is 1/4 of those in ImageNet, i.e., the channels increase from 16 to 128. We initialize expansion ratio uniformly at 1.5 for DMS-A and 2.5 for DMS-B. σ is initialized uniformly to 1 and progressively decreased to 0.3 at the end of the search. This initialization ensures expansion ration has same explore space in the beginning of the search. In our search space, we set the minimum expansion ratio to 0.3 and the minimum $\mu - \Delta$ is 0.25. We do not set upper bound for expansion ratio, which means our search space is infinite. We also match the target memory to its corresponding 1x or 3x BNN. In particular, the target memory is set to 0.12, 1 for DMS-A and DMS-B. Half of the training data are held out as validation data, which is the same with DARTS. Total training epoch is set to 250, and we optimize μ for every 5 epochs training of weights. Batch size is set to 64 for both training and validation. SGD with momentum of 0.9 is adopted to optimize the weights, where the learning rate is set to 0.05 and annealed to 0.01 with a cosine schedule (Loshchilov & Hutter, 2016) in every 5 epochs.

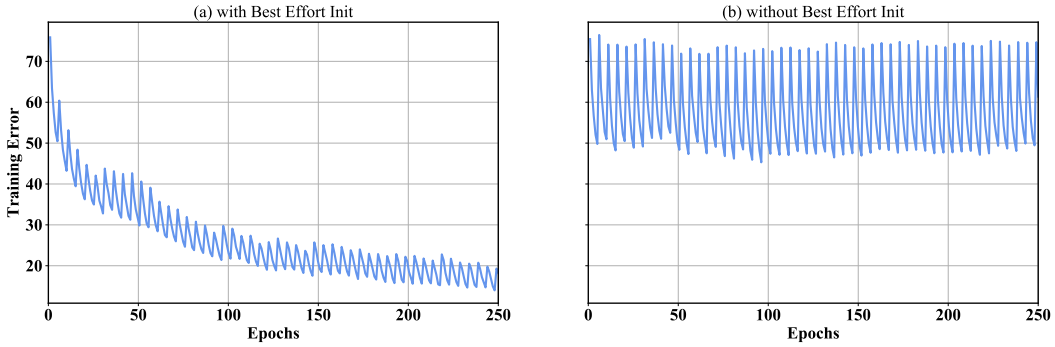

Figure 3: Training errors during searching. We show model without best effort initialization cannot converge.

Adam Kingma & Ba (2014) optimizer is adopted when descending validation loss and the learning rate is set to 2×10^{-3} for VGG and 1×10^{-3} for ResNet. Weight decay is set to 10^{-4} and the tradeoff parameter λ is set to 0.01. We do not use Gumbel ST when sampling the convolution layer with different dimension. The temperature τ is set to 1 as an constant. The search algorithm only takes 2-4 hours on a single NVIDIA GTX 1080Ti GPU.

B.2.2 Network Evaluation

For CIFAR10 experiments, we directly use the optimized μ for the expansion ratio when evaluating a model. VGG models are trained from scratch with SGD optimizer. Momentum is set to 0.9. We train the model for 300 epochs, the learning rate is initialized to 0.1 and decayed with a factor of 0.1 at epoch 140, 220 and 260. Weight decay is set to 10^{-4} for DMS-A and 2×10^{-4} for DMS-B. For ResNet-18, we first train the full precision model for 200 epochs and then we use the full precision model to initialize BNN. Other configuration is the same with VGG training.

For ImageNet dataset, we directly apply the model searched on CIFAR-10 and trained it for 100 epochs with the same hyperparameter setting as the original ResNet-18. Then the binarized version is trained with it as an initialization. The learning rate is set to ... and decayed with a cosine learning rate scheduler.

B.2.3 BNN Settings

We use the binarization introduced in XNOR-Net (Rastegari et al., 2016) for weights. Before weight binarization, we apply Weight Standardization (Qiao et al., 2019) to normalize each filter to zero mean and unit variance. For activations binarization, the quantization step α is jointly optimized with network parameters. We do not quantize the first and the last layers following the prior implementation (Zhou et al., 2016).

B.3 Channel Distribution

We envision the channel numbers of our DMS searched architecture on VGG-11 and ResNet-18 in Fig. 4. Conventional architecture design tends to progressively increase the channel numbers as the layers go deep. However, recent research (He et al., 2017) on structured pruning shows channels are redundant in full precision neural networks. This redundancy may also exist when we want to widen the layers, typically in BNN. First, in Fig. 4a, we notice that the fourth and sixth layer DMS architecture is extremely pruned, indicating these two layers may contain redundant information even when activations are binarized. Whereas the first three layer are more favorable by our search algorithm. In ResNet-18, we also notice that the discrepancies of expansion ratio result in higher accuracy.

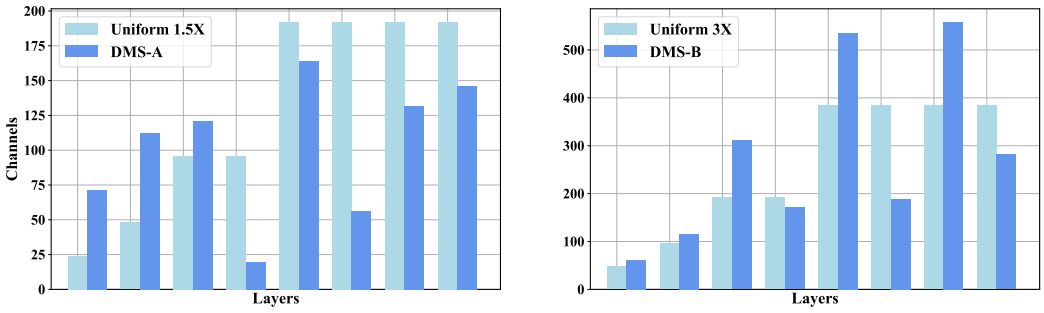

(a) Channel distribution for ResNet-18.

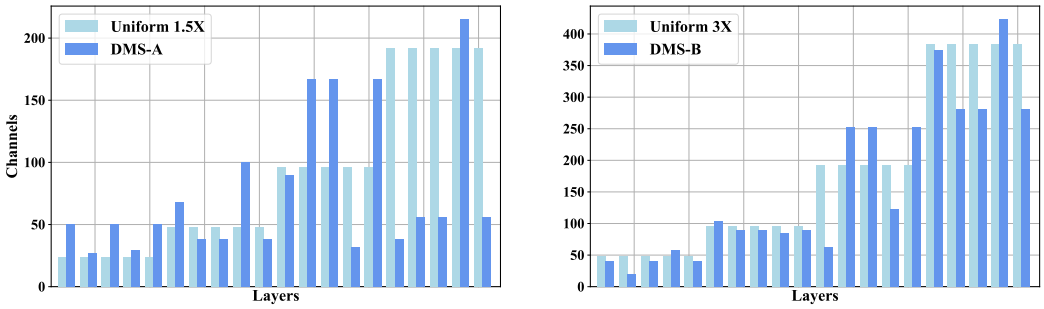

(b) Channel distribution for VGG-11.

Figure 4: Comparison of channel numbers between wide BNN and our DMS architecture.